Discovery potential for supersymmetry at a high luminosity upgrade of LHC14

Howard Baer,[1,*] V. Barger,[2,†] Andre Lessa,[3,‡] and Xerxes Tata[4,§]

[1]*Department of Physics and Astronomy, University of Oklahoma, Norman, Oklahoma 73019, USA*
[2]*Physics Department, University of Wisconsin, Madison, Wisconsin 53706, USA*
[3]*Instituto de Física, Universidade de São Paulo, São Paulo, São Paulo, Brazil*
[4]*Department of Physics and Astronomy, University of Hawaii, Honolulu, Hawaii 96822, USA*

(Received 30 July 2012; published 3 December 2012)

After completion of the LHC8 run in 2012, the plan is to upgrade the LHC for operation close to its design energy $\sqrt{s} = 14$ TeV, with a goal of collecting hundreds of fb^{-1} of integrated luminosity. The time is propitious to begin thinking of what is gained by even further LHC upgrades. In this report, we compute an LHC14 reach for supersymmetry in the mSUGRA/CMSSM model with an anticipated high luminosity upgrade. We find that LHC14 with 300 (3000) fb^{-1} has a reach for supersymmetry via gluino/squark searches of $m_{\tilde{g}} \sim 3.2$ TeV (3.6 TeV) for $m_{\tilde{q}} \sim m_{\tilde{g}}$, and a reach of $m_{\tilde{g}} \sim 1.8$ TeV (2.3 TeV) for $m_{\tilde{q}} \gg m_{\tilde{g}}$. In the case where $m_{\tilde{q}} \gg m_{\tilde{g}}$, then the LHC14 reach for chargino-neutralino production with decay into the $Wh + \not{E}_T$ final state reaches to $m_{\tilde{g}} \sim 2.6$ TeV for 3000 fb^{-1}.

DOI: 10.1103/PhysRevD.86.117701 PACS numbers: 14.80.Ly, 12.60.Jv, 13.85.Qk

I. INTRODUCTION

The LHC collider has delivered ~5 fb^{-1} of integrated luminosity at $\sqrt{s} = 7$ TeV (LHC7), and so far over 6 fb^{-1} at 8 TeV (LHC8). These runs have met with great success as evidenced by a 5σ discovery of a Higgs-like particle with $m_h \sim 125$ GeV. So far, no direct sign of supersymmetry (SUSY) has emerged, leading to mass limits in the mSUGRA/CMSSM model [1] of $m_{\tilde{g}} \gtrsim 1.4$ TeV for $m_{\tilde{q}} \simeq m_{\tilde{g}}$ and $m_{\tilde{g}} \gtrsim 0.85$ TeV for $m_{\tilde{q}} \gg m_{\tilde{g}}$ based on analyses of just LHC7 data. The LHC expects to continue running through the remainder of 2012 with a goal of collecting ~20 fb^{-1} at 8 TeV. In 2013–2014, the LHC is expected to be shut down for an energy upgrade, with running sets to resume around 2015 with $\sqrt{s}$ close to the LHC design energy of 14 TeV. The goal then is to amass an order of hundreds of fb^{-1} of integrated luminosity at LHC14.

Planning has already begun for further upgrades beyond LHC14 with a design luminosity ~100 fb^{-1}/yr. One option is a possible energy upgrade, which would require design, construction, and deployment of a completely new set of magnets. A more economical (and perhaps technologically viable) alternative may be a luminosity upgrade, with the possible target of gathering ~3000 fb^{-1} of integrated luminosity. In this short article, we try to quantify the increased reach of LHC for SUSY if the total integrated luminosity is increased from 300 to 3000 fb^{-1}. While the increasing sparticle mass limits from LHC seem to make the mSUGRA model increasingly implausible (in light of fine-tuning considerations), nonetheless we continue to work in this paradigm case mainly for historical reasons. Moreover, many physicists are familiar with the m_0 vs $m_{1/2}$ plane of this model; it is easy to compare with projections from previous studies [2–5] and many current analyses of data [6,7] continue to be presented in this framework. In particular, in Ref. [5], the projected reach of LHC7 for 5–30 fb^{-1} was calculated. The increase in beam energy to 8 TeV should lead to a modest increase of expected reach beyond these results. Drawing upon these results, we estimate that the LHC8 with 20 fb^{-1} will probe out to $m_{\tilde{g}} \sim 1.8$ TeV for $m_{\tilde{q}} \simeq m_{\tilde{g}}$ and to $m_{\tilde{g}} \sim 1$ TeV for $m_{\tilde{q}} \gg m_{\tilde{g}}$. At LHC14 with 100 fb^{-1}, the gluino reach extends to 3.0 TeV if $m_{\tilde{q}} \simeq m_{\tilde{g}}$.

The preceding LHC reach results have been obtained by looking for signatures arising from gluino and squark pair production reactions followed by cascade decays [8], leading to multijet plus missing E_T ($\not{E}_T$) signatures along with possibly one or more isolated leptons.[1] It has been pointed out long ago and emphasized more recently that in models with gaugino mass unification, as higher sparticle masses are probed, ultimately chargino and neutralino pair production reactions will dominate over gluino and squark pair production. In these models—where $|\mu|$ is assumed much greater than gaugino masses M_1 and M_2 and where $m_{\tilde{q}} \gg m_{\tilde{g}}$ with $m_{\tilde{g}} \gtrsim 1$ TeV—the gaugino production process, $pp \to \tilde{W}_1\tilde{Z}_2$, tends to be the dominant sparticle production cross section at LHC. At such high masses, the dominant decay modes tend to be $\tilde{W}_1 \to W\tilde{Z}_1$ and $\tilde{Z}_2 \to \tilde{Z}_1 h$ (also with some non-negligible fraction of $\tilde{Z}_2 \to \tilde{Z}_1 Z$ decays). This has led some groups to consider the LHC reach in the $pp \to \tilde{W}_1\tilde{Z}_2 \to W(\to l\nu) + h(\to b\bar{b}) + \not{E}_T$ channel [10].

In this article, we will consider both the gluino and squark cascade decay signatures and the $Wh + \not{E}_T$

*baer@nhn.ou.edu
†barger@pheno.wisc.edu
‡lessa@fma.if.usp.br
§tata@phys.hawaii.edu

[1]Tagging of b jets may potentially increase the LHC14 reach from above projections by as much as 20% in the so-called HB/FP region of parameter space [9].

 © 2012 American Physical Society

channel. A major problem in assessing the LHC reach for extremely high integrated luminosity projections is to gain reasonable background estimates from standard model (SM) processes. As higher sparticle masses are probed, harder jet and $\not{E}_T$ and other cuts are designed to maximize the reach for signal against background. With hard enough cuts, the expected SM background rates may drop into the tens of events level, requiring simulations with up to billions of events to attain the needed statistical accuracy. Such large Monte Carlo samples are highly time and space intensive at present. Thus, in the case of very hard cuts, here we resort to fits of SM background projections which we hope will be within factors of a few times the real result. We show details of our background and signal generation in Sec. II, along with our fits which are needed for very hard cuts. In Sec. III we conclude and summarize our results.

II. LHC14 REACH FOR SUSY WITH 300 fb^{-1} AND 3000 fb^{-1}

For the simulation of the background events, we use ALPGEN [11] to compute the hard scattering events and PYTHIA [12] for the subsequent showering and hadronization. The standard model background simulation details follows closely to the discussion in Ref. [3], so we do not reproduce them here. The only difference is the inclusion of the $W(\rightarrow l\nu) + h$, $Z(\rightarrow l^+l^-) + h$ and $t\bar{t} + h$ processes, where we take $m_h = 125$ GeV. The signal events were generated using Isajet 7.82 [13]. We assume the mSUGRA (CMSSM) framework [1] with $\tan\beta = 10$, $\mu > 0$ and $A_0 = -2m_0$; such a large negative A_0 value ensures that $m_h \sim 123$–127 GeV throughout most of mSUGRA parameter space [14]. All $2 \rightarrow 2$ SUSY production processes are included at leading order. To simulate detector efficiencies and smearing, we use the toy detector simulation described in Ref. [3]. We assume the same detector parameters (including b-tag efficiency) for the 300 and 3000 fb^{-1} scenarios. Jets and isolated lepton are defined as follows:

(i) Jets are hadronic clusters with $|\eta| < 3.0$, $R \equiv \sqrt{\Delta\eta^2 + \Delta\phi^2} \leq 0.4$ and $E_T(\text{jet}) > 50$ GeV.

(ii) Electrons and muons are considered isolated if they have $|\eta| < 2.0$, $p_T(l) > 10$ GeV with visible activity within a cone of $\Delta R < 0.2$ about the lepton direction, $\Sigma E_T^{\text{cells}} < 5$ GeV.

(iii) We identify hadronic clusters as b-jets if they contain a B hadron with $E_T(B) > 15$ GeV, $\eta(B) < 3$, and $\Delta R(B, \text{jet}) < 0.5$. We assume a tagging efficiency of 60% and light quark and gluon jets can be mistagged as a b jet with a probability $1/150$ for $E_T \leq 100$ GeV, $1/50$ for $E_T \geq 250$ GeV, with a linear interpolation for $100\ \text{GeV} \leq E_T \leq 250$ GeV [15] in between.

In order to address the discovery potential for distinct signal topologies, we investigate four different channels:

(i) $0l$: $n(l) = 0$, $n(j) \geq 3$, $\{E_T(j_1), E_T(j_2), E_T(j_3)\} > \{100, 100, 50\,\text{GeV}\}$,

(ii) $1l$: $n(l) = 1$, $n(j) \geq 2$, $\{E_T(j_1), E_T(j_2)\} > \{100, 100\ \text{GeV}\}$,

(iii) $2l$: $n(l) = 2$, $n(j) \geq 2$, $\{E_T(j_1), E_T(j_2)\} > \{300, 300\ \text{GeV}\}$,

(iv) Wh: $n(l) = 1$, $n(b) = n(j) = 2$, $\Delta\phi(b, b) < \pi/2$, $M_{\text{eff}} > 350$ GeV, $m_T > 125$ GeV, $100\ \text{GeV} < m_{bb} < 130$ GeV,

where $n(l)$ is the number of isolated leptons (electrons and muons), $n(j)$ is the number of jets (including b jets), $E_T(j_i)$ is the transverse energy of the ith jet, $n(b)$ is the number of b-tagged jets, $\Delta\phi(b, b)$ is the azimuthal angle separation between two b jets, $M_{\text{eff}} = \sum_i E_T(j_i) + \sum_i p_T(l_i) + \not{E}_T$, m_T is the transverse mass and m_{bb} the invariant mass of the b jet pair. While the $0l$, $1l$, and $2l$ channels focus mostly on signal topologies from gluino and squark production and cascade decay, the Wh channel targets $\tilde{W}_1\tilde{Z}_2$ production, with $\tilde{W}_1 \rightarrow W + \tilde{Z}_1$ and $\tilde{Z}_2 \rightarrow h + \tilde{Z}_1$, as discussed in Ref. [10].[2] Although these channels do not necessarily give the maximum reach in all regions of parameter space, they are inclusive enough to discuss the gain of a luminosity upgrade.

For each of the above channels, we plot the SM background and signal $\not{E}_T$ distributions and verify if the signal is visible for $\not{E}_T > \not{E}_{T\text{cut}}$, where the value of $\not{E}_{T\text{cut}}$ is allowed to vary in the interval 0.1–1.5 TeV (in steps of 0.1 TeV). We deem that the signal is visible if there is a value of $\not{E}_{T\text{cut}}$ such that, for $\not{E}_T > \not{E}_{T\text{cut}}$, the signal satisfies:

$$SG \geq \max[5\ \text{events}, 0.2\text{BG}, 5\sqrt{\text{BG}}], \tag{2.1}$$

where SG (BG) is the number of signal (background) events for a given integrated luminosity.

Since $\not{E}_{T\text{cut}}$ can be as large as 1.5 TeV, there are large Monte Carlo (MC) statistical uncertainties for such hard cuts, due to the limited number of events in our background MC samples. To reduce these uncertainties, we *extrapolate* the background to large $\not{E}_T$. Since we will eventually require $\not{E}_T > \not{E}_{T\text{cut}}$, it is more convenient to consider the *cumulative* $\not{E}_T$ distribution, defined by

$$\sigma(S_{\text{miss}}) \equiv \int_{S_{\text{miss}}}^{\infty} \frac{d\sigma}{d\not{E}_T} d\not{E}_T. \tag{2.2}$$

Thus, the total cross section for $\not{E}_T > \not{E}_{T\text{cut}}$ is simply $\sigma(S_{\text{miss}} = \not{E}_{T\text{cut}})$. Furthermore, if $d\sigma/d\not{E}_T$ falls exponentially, so does $\sigma(S_{\text{miss}})$. Therefore, we extrapolate the $\sigma(S_{\text{miss}})$ distribution to large S_{miss} values, assuming an exponential shape at large S_{miss}. The extrapolation of $\sigma(S_{miss})$ instead of $d\sigma/d\not{E}_T$ reduces the MC uncertainties, since the former is a cumulative function. As an example

[2]In the present study we have included the important $Z(\rightarrow \nu\bar{\nu})t\bar{t}$ background, which was not included in Ref. [10], but becomes relevant for hard $\not{E}_T$ cuts.

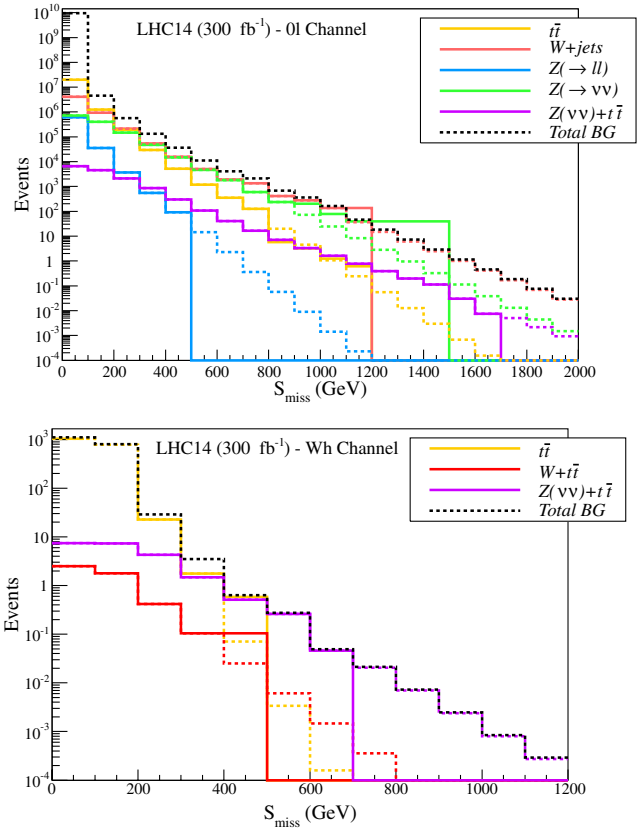

FIG. 1 (color online). Cumulative $\not{E}_T$ distributions ($S_{\rm miss}$) for the dominant SM backgrounds in the $0l$ (top panel) and Wh (bottom panel) channels defined in the text. We assume $\sqrt{s} = 14$ TeV and an integrated luminosity of 300 fb^{-1}. The solid lines represent the distributions from our MC samples, while the dashed lines show the extrapolated distribution used in our analysis, as discussed in the text. Only the dominant SM processes are shown. The black dashed line shows the total extrapolated background, which includes all SM processes.

we show the $S_{\rm miss}$ distribution before and after the extrapolation for the $0l$ and Wh channels in Fig. 1. As we can see, this extrapolation procedure allows us to consider hard $\not{E}_T$ cuts, which are essential for isolating the signal at high integrated luminosities.

Using the four channels listed above, as well as the extrapolated SM background, we estimate the discovery potential for supersymmetry assuming 300 and 3000 fb^{-1} of integrated luminosity. We present our results in the m_0 vs $m_{1/2}$ plane and consider the $0l$, $1l$, $2l$, and Wh channels separately. We deliberately do not show results for the rate-limited but relatively background-free same-sign dilepton and trilepton channels, because we were unable to reliably estimate the backgrounds for these high values of integrated luminosity. Also, hard-to-estimate lepton fakes could make substantial contributions to the background.

Our results are shown in Fig. 2, where the solid lines show the reach in each channel for 300 fb^{-1}, while the dashed lines correspond to the 3000 fb^{-1} reach. The lower-left shaded region is excluded by SUSY searches at LHC7 using ~5 fb^{-1} of data [6,7].

For an integrated luminosity of 300 fb^{-1}, we see from Fig. 2 that the $0l$ channel gives the maximum reach for small m_0 values, where $m_{\tilde{g}} \sim m_{\tilde{q}}$. In this case the reach goes up to $m_{\tilde{g}} \sim 3.2$ TeV. For higher m_0 values, where $m_{\tilde{g}} \ll m_{\tilde{q}}$, the maximum reach is obtained in the $1l$ and $2l$ channels and extends to $m_{\tilde{g}} \sim 1.8$ TeV. At these mass scales, the $\tilde{W}_1\tilde{Z}_2 \to Wh + \not{E}_T$ channel gives a much smaller reach at 300 fb^{-1}, going up to $m_{\tilde{g}} \sim 1.2$ TeV in the squark decoupling limit.

This picture significantly changes if we assume a high integrated luminosity of 3000 fb^{-1}. In this case, channels with smaller signal cross sections, but larger signal/background ratios, such as the $1l$, $2l$, and Wh channels, provide the maximum reach for most of the parameter space. For $m_{\tilde{q}} \sim m_{\tilde{g}}$, the reach is dominated by the $0l$ and $1l$ channels and goes up to $m_{\tilde{g}} \sim 3.6$ TeV. For $m_0 \gtrsim 3$ TeV, where squarks start to decouple, the maximum reach is obtained in the Wh channel, since, for $m_{\tilde{g}} \gtrsim 2$ TeV, electroweak gaugino production overcomes gluino production by almost an order of magnitude.

We see from Fig. 2 that for an integrated luminosity of 300 (3000) fb^{-1}, the reach in the Wh channel for $m_{\tilde{g}} \ll m_{\tilde{q}}$ extends to $m_{1/2} \sim 550$ GeV (1150 GeV) corresponding to $m_{\tilde{W}_1} \sim 450$ GeV (950 GeV). This reach corresponds to gluino masses of up to ~1.2 (2.6) TeV. Although these numbers superficially seem lower than our earlier projections [10], we should keep in mind that here we have not

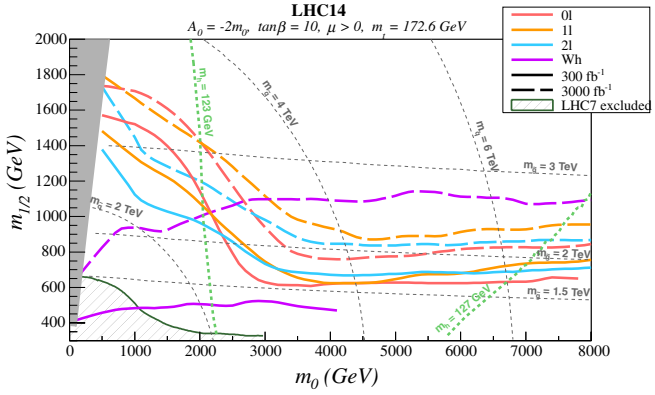

FIG. 2 (color online). SUSY reach in the four channels discussed in the text for LHC14 for integrated luminosities of 300 fb^{-1} (solid lines) and 3000 fb^{-1} (dashed lines). The signal is observable if it falls below the curve for the corresponding integrated luminosity. The fixed mSUGRA parameters are $A_0 = -2m_0$, $\tan\beta = 10$ and $\mu > 0$. Gluino and squark mass contours are shown by the dashed, dark grey curves. We also show contours of $m_h = 123$ and 127 GeV. The shaded grey area on the left side of the figure is excluded because the stau becomes the LSP. The green shaded region in lower-left is excluded by SUSY searches at LHC7.

TABLE I. The choice of the $\not{E}_T$ cut variable $S_{\rm miss}$ introduced in Eq. (2.2) used to optimize the signal in the various channels shown in Fig. 2, the cross sections in fb for the main SM backgrounds as well as for the sample mSUGRA point $m_0 = 5$ TeV, $m_{1/2} = 750$ GeV, $A_0 = -2m_0$, $\tan\beta = 10$, and $\mu > 0$.

	0ℓ	1ℓ	2ℓ	Wh
$S_{\rm miss}$ (TeV)	1.1	1	0.7	0.3
$t\bar{t}$	8.0×10^{-4}	9.3×10^{-3}	1.9×10^{-2}	5.9×10^{-3}
$W + j$	1.2×10^{-1}	5.2×10^{-2}	0	0
$Z(\rightarrow \ell\bar{\ell}) + j$	7.6×10^{-7}	1.0×10^{-3}	0	0
$Z(\rightarrow \nu\bar{\nu}) + j$	2.8×10^{-2}	3.9×10^{-4}	0	0
$Z(\rightarrow \nu\bar{\nu}) + t\bar{t}$	2.6×10^{-3}	1.4×10^{-3}	2.0×10^{-3}	4.9×10^{-3}
$Wt\bar{t}$	7.0×10^{-4}	3.5×10^{-4}	1.8×10^{-4}	3.5×10^{-4}
Total background	0.15	0.07	0.02	0.01
SUGRA	0.04	0.04	0.02	0.02

included any signal K factors and have also included the $Zt\bar{t}$ background. We note, however, that the renormalization/factorization scale used here for the background processes is such that the $t\bar{t}$ total cross section is normalized to its next-to-leading order value (for more details see Ref. [3]).

We recall that to obtain the reach shown in Fig. 2 above, in addition to the channel-dependent cuts on jets and leptons listed earlier, we have required an additional cut $\not{E}_T > S_{\rm miss}$ [see Eq. (2.2)]. Then, for each channel and for each grid point in the $m_0 - m_{1/2}$ plane, we have chosen the value of $S_{\rm miss}$ to optimize the observability of the signal relative to the SM background obtained using the extrapolated $\not{E}_T$ spectrum discussed above. In Table I we show the signal cross section for the mSUGRA model point $m_0 = 5$ TeV, $m_{1/2} = 750$ GeV, $A_0 = -2m_0$, $\tan\beta = 10$, and $\mu > 0$ along with the cross section for the various background components along with the chosen value of $S_{\rm miss}$. The signal case is chosen because it requires an ab^{-1} scale integrated luminosity for observability. We emphasize that the backgrounds depend strongly on $S_{\rm miss}$, and so vary depending on where we are in the $m_0 - m_{1/2}$ plane.

In Fig. 3, we show the combined SUSY reach contours for LHC14 with 100, 300, 1000, and 3000 fb^{-1} of integrated luminosity.[3] The points below each curve are considered observable if they are observable in at least one of the previously discussed four channels. The kink in each of the 1000 and 3000 fb^-1 curves near $m_0 \simeq 3$–3.5 TeV occurs because the Wh signal channel allows one to probe larger $m_{1/2}$ than those accessible via gluino cascade decays.

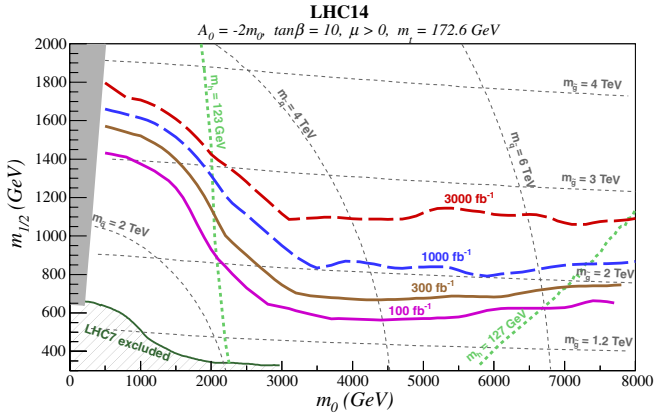

FIG. 3 (color online). SUSY reach in the *combined* four channels as discussed in the text for LHC14 for integrated luminosities of 100, 300, 1000, and 3000 fb^{-1}. The signal is observable if it falls below the curve for the corresponding integrated luminosity. The fixed mSUGRA parameters are $A_0 = -2m_0$, $\tan\beta = 10$ and $\mu > 0$. Gluino and squark mass contours are shown by the dashed, dark grey curves. We also show contours of $m_h = 123$ and 127 GeV. The shaded grey area on the left side of the figure is excluded because the stau becomes the LSP. The lower-left shaded region is excluded by SUSY searches at LHC7.

III. CONCLUSIONS

In this study we have investigated the discovery potential of possible high luminosity upgrades of LHC14 for supersymmetry within the mSUGRA/CMSSM framework. Previous reach projections for high integrated luminosity values were presented in Ref. [3]. In the current paper we have made improved background projections/extrapolations involving the cases where very hard cuts severely limit the statistical accuracy of the background estimate. We have updated our mSUGRA projections with $A_0 \sim -2m_0$ so that the value of m_h is close to 125 GeV throughout most of parameter space. Third, we have included the reach projection from $pp \rightarrow \tilde{W}_1\tilde{Z}_2 \rightarrow Wh + \not{E}_T$ which

[3]Aside from the theoretical difficulties of calculating the backgrounds for the very hard cuts considered here, we also note that for our projections we have assumed that detector resolutions and b jet tagging will remain close to their present values even in the high luminosity environment, and that event pileup (which depends on the details of the beam) will not be an issue.

TABLE II. Optimized SUSY reach of LHC14 within the mSUGRA model expressed in terms of $m_{\tilde{g}}$ for various choices of integrated luminosity. The $m_{\tilde{q}} \sim m_{\tilde{g}}$ and $m_{\tilde{q}} \gg m_{\tilde{g}}$ values correspond to the maximum reach in the $0l$, $1l$, and $2l$ channels, while the Wh values correspond to the reach in the Wh channel for $m_{\tilde{q}} \gg m_{\tilde{g}}$.

IL (fb^{-1})	$m_{\tilde{q}} \sim m_{\tilde{g}}$ (TeV)	$m_{\tilde{q}} \gg m_{\tilde{g}}$ (TeV)	Wh
100	3.0	1.6	- TeV
300	3.2	1.8	1.2 TeV
1000	3.4	2.0	2.0 TeV
3000	3.6	2.3	2.6 TeV

should give the dominant SUSY reach channel for $m_{\tilde{q}} \gg m_{\tilde{g}}$ and very high integrated luminosity.

Our final reach projections listed in terms of $m_{\tilde{g}}$ in TeV units are summarized in Table II for several integrated luminosity values. We find that LHC14 with 300 (3000) fb^{-1} has a reach for SUSY via gluino/squark searches of $m_{\tilde{g}} \sim 3.2$ TeV (3.6 TeV) for $m_{\tilde{q}} \sim m_{\tilde{g}}$, and a reach of $m_{\tilde{g}} \sim 1.8$ TeV (2.3 TeV) for $m_{\tilde{q}} \gg m_{\tilde{g}}$. In the case where $m_{\tilde{q}} \gg m_{\tilde{g}}$, the reach is higher in the Wh channel, going up to $m_{\tilde{g}} \sim 2.6$ TeV for 3000 fb^{-1}. We point out that the reach in this channel is only related to $m_{\tilde{g}}$ through the gaugino mass unification assumption, since the Wh channel depends only on the $pp \to \tilde{W}_1 \tilde{Z}_2$ production cross section and the subsequent cascade decays. For models where gaugino unification is not assumed, the reach is independent of $m_{\tilde{g}}$ and goes up to $m_{\tilde{W}_1} \sim 450$ GeV (950 GeV), for 300 fb^{-1} (3000 fb^{-1}) and $M_1 \leq M_2 \ll \mu$.

ACKNOWLEDGMENTS

We thank A. Barr and A. Nisati for comments on the manuscript. We thank the Center for Theoretical Underground Physics and Related Areas (CETUP* 2012) in South Dakota for its hospitality and for partial support during the completion of this work. This research was supported in part by grants from the United States Department of Energy and Fundacão de Apoio à Pesquisa do Estado de São Paulo (FAPESP).

[1] A. Chamseddine, R. Arnowitt, and P. Nath, Phys. Rev. Lett. **49**, 970 (1982); R. Barbieri, S. Ferrara, and C. Savoy, Phys. Lett. **119B**, 343 (1982); N. Ohta, Prog. Theor. Phys. **70**, 542 (1983); L. Hall, J. Lykken, and S. Weinberg, Phys. Rev. D **27**, 2359 (1983); for a review, see, e.g., P. Nath, arXiv:hep-ph/0307123, and references therein.

[2] H. Baer, X. Tata, and J. Woodside, Phys. Rev. D **45**, 142 (1992); H. Baer, C. H. Chen, F. Paige, and X. Tata, Phys. Rev. D **52**, 2746 (1995); **53**, 6241 (1996); H. Baer, C. H. Chen, M. Drees, F. Paige, and X. Tata, Phys. Rev. D **59**, 055014 (1999); H. Baer, C. Balázs, A. Belyaev, T. Krupovnickas, and X. Tata, J. High Energy Phys. 06 (2003) 054; see also S. Abdullin and F. Charles, Nucl. Phys. **B547**, 60 (1999); S. Abdullin *et al.* (CMS Collaboration), J. Phys. G **28**, 469 (2002); B. Allanach, J. Hetherington, A. Parker, and B. Webber, J. High Energy Phys. 08 (2000) 017.

[3] H. Baer, V. Barger, A. Lessa, and X. Tata, J. High Energy Phys. 09 (2009) 063.

[4] H. Baer, V. Barger, A. Lessa, and X. Tata, J. High Energy Phys. 06 (2010) 102.

[5] H. Baer, V. Barger, A. Lessa, and X. Tata, Phys. Rev. D **85**, 051701 (2012).

[6] G. Aad *et al.* (ATLAS collaboration), Phys. Lett. B **710**, 67 (2012); see M. Backes, in ICHEP, Melbourne, Australia, 2012 (unpublished), for a recent update.

[7] S. Chatrchyan *et al.* (CMS collaboration), Phys. Rev. Lett. **107**, 221804 (2011); see S. Sharma, in ICHEP, Melbourne, Australia, 2012 (unpublished), for a recent update.

[8] H. Baer, J. Ellis, G. Gelmini, D. V. Nanopoulos, and X. Tata, Phys. Lett. **161B**, 175 (1985); G. Gamberini, Z. Phys. C **30**, 605 (1986); H. Baer, V. Barger, D. Karatas, and X. Tata, Phys. Rev. D **36**, 96 (1987); H. Baer, R. M. Barnett, M. Drees, J. F. Gunion, H. E. Haber, D. L. Karatas, and X. R. Tata, Int. J. Mod. Phys. A **02**, 1131 (1987); R. M. Barnett, J. F. Gunion, and H. E. Haber, Phys. Rev. D **37**, 1892 (1988); H. Baer, A. Bartl, D. Karatas, W. Majerotto, and X. Tata, Int. J. Mod. Phys. A **04**, 4111 (1989); H. Baer, X. Tata, and J. Woodside, Phys. Rev. D **42**, 1568 (1990); A. Bartl, W. Majerotto, B. Mosslacher, N. Oshimo, and S. Stippel, Phys. Rev. D **43**, 2214 (1991); A. Bartl, W. Majerotto, and W. Porod, Z. Phys. C **64**, 499 (1994).

[9] P. Mercadante, J. Mizukoshi, and X. Tata, Phys. Rev. D **72**, 035009 (2005); S. P. Das, M. Guchait, M. Maity, and S. Mukherjee, Eur. Phys. J. C **54**, 645 (2008); R. H. K. Kadala, P. G. Mercadante, J. K. Mizukoshi, and X. Tata, Eur. Phys. J. C **56**, 511 (2008).

[10] H. Baer, V. Barger, A. Lessa, W. Sreethawong, and X. Tata, Phys. Rev. D **85**, 055022 (2012); D. Ghosh, M. Guchait, and D. Sengupta, Eur. Phys. J. C **72**, 2141 (2012).

[11] M. Mangano, M. Moretti, F. Piccinini, R. Pittau, and A. Polosa, J. High Energy Phys. 07 (2003) 001.

[12] T. Sjostrand, S. Mrenna, and P. Skands, J. High Energy Phys. 05 (2006) 026.

[13] ISAJET, by H. Baer, F. Paige, S. Protopopescu, and X. Tata, arXiv:hep-ph/0312045.

[14] H. Baer, V. Barger, P. Huang, and A. Mustafayev, Phys. Rev. D **84**, 091701 (2011); H. Baer, V. Barger, and A. Mustafayev, Phys. Rev. D **85**, 075010 (2012).

[15] S. Corréad, V. Kostioukhine, J. Levêque, A. Rozanov, and J. B. de Vivie, ATLAS Report No. ATLAS-PHYS-2004-006; V. Kostioukhine, ATLAS Report No. ATLAS-PHYS-2003-033.